Multiphysics Modelling of Food Dehydration during RF Exposure

Ryan Renshaw
*Corresponding author: 106 Waterhouse Lane, Chelmsford, Essex, UK, CM1 2QU,
ryan.renshaw@e2v.com

Abstract: There is a requirement for an RF industrial dryer, that will be capable of dehydrating foodstuff to the correct level after the product has been fried.

RF drying should actively target moisture, due to waters high dielectric properties. An industrial dryer can be optimised using modelling to obtain the correct moisture removal rates in the RF drying process.

Measurement of the dielectric properties was carried out at varying moisture levels to obtain the correct dielectric material properties for this model.

The foodstuff can be accurately described as porous media. The model essentially describes dehydration of the foodstuff through evaporation and transport phenomena, driven by RF heating. This paper describes the initial 2D model used to capture all the physics. The 2D model enabled quick turn around of sensitivity studies used to validate model behaviour. It was also used as a test bed for future idealisations.

The methodology presented in this report will be used to generate a full 3D model of the industrial dryer.

Keywords: RF, drying, dehydration, foodstuffs

1. Introduction

This paper presents a fully coupled 2D multiphysics model of a porous media food being dehydrated using RF exposure. RF heating should decrease sharply as water content decreases. Hence, the RF heating will target high levels of moisture. This effect can ultimately be modelled to specify an optimised RF industrial dryer that would be capable of dehydrating food without exceeding critical temperatures.

2. Governing Equations and theory

The application modes used in the 2D model are as follows:

- Incompressible Navier stokes for free air flow outside Porous media
- Darcy's Law for flow inside Porous media
- Convection and diffusion to describe water, vapour and oil inside the Porous media
- Convection and diffusion to describe vapour flow in free air outside the porous media
- Convection and conduction to describe heat transfer
- In-Plane TE Waves for the RF analysis

The model included the following fluids:

- Porous food material
- Air
- Water
- Water vapour
- Oil

A number of additional expressions had to be entered into the model to fully describe the physics. The equations used for each fluid is presented in the following subsections

The methodology presented in this section of the paper was developed in conjunction with Peter Yakubenko of Comsol (see the acknowledgement section and reference 1).

2.1 Gas transport equations within porous media

Darcy's Law is used within the food porous media, as described in Equation 1. This is built into the Darcy's Law application mode in the Chemical Engineering Module.

$$\frac{\partial \varepsilon S_g \rho_g}{\partial t} + \nabla\left(-\rho_g \frac{\kappa_g}{\eta_g}\nabla P\right) = F \quad \text{Eq. 1}$$

A number of the terms in Equation 1 are not constant in this analysis, and were entered as "scalar expressions".

The gas, water and oil saturation levels are presented in Equations 2, 3 and 4 respectively.

$$S_g = 1 - S_w - S_o \quad \text{Eq. 2}$$

$$S_w = \frac{C_w}{\rho_w \varepsilon} \quad \text{Eq. 3}$$

$$S_o = \frac{C_o}{\rho_o \varepsilon} \quad \text{Eq. 4}$$

Equations 3 and 4 require water and oil mass concentration, which is presented in Equations 5 and 6 respectively.

$$C_w = c_w \overline{m_w} \quad \text{Eq. 5}$$

$$C_o = c_o \overline{m_o} \quad \text{Eq. 6}$$

Darcy's law (Equation 1), also required input for permeability of air in the food. This expression was taken from reference 2 and is presented in Equation 7.

$$\kappa_g = \kappa_{gi} \kappa_{gr} \quad \text{Eq. 7}$$

The relative permeability is presented in Equation 8 and 9, again taken from reference 2. Intrinsic permeability is a constant.

$$\kappa_{gr} = 1 - 1.1 S_w \text{ when } S_w < \frac{1}{1.1} \quad \text{Eq. 8}$$

$$\kappa_{gr} = 0 \text{ when } S_w > \frac{1}{1.1} \quad \text{Eq. 9}$$

Vapour is added to the gas within the porous media as the water evaporates during RF heating. Therefore evaporation, described in Equation 10, is entered into the source term for Darcy's Law (equation 1).

$$\dot{m} = K \frac{\overline{m_w}}{RT} \left(P_{v,eq} - P_v \right) \quad \text{Eq. 10}$$

The equation for Vapour equilibrium pressure is presented in Equation 11. The corresponding set of equations for Vapour saturated partial pressure and water activity were taken from reference 3 (they are not presented in this paper).

$$P_{v,eq} = P_{v,sat} a_w \quad \text{Eq. 11}$$

The Water Activity Sorption equations require the moisture content, as described in Equation 12. This is also a very useful measure for postprocessing.

$$X_m = \frac{C_w}{(1-\varepsilon)\rho_s} \quad \text{Eq. 12}$$

The Vapour partial pressure used to calculate evaporation rate (Equation 10) is presented in Equation 13.

$$P_v = \frac{C_v RT}{\varepsilon S_g \overline{m_w}} \quad \text{Eq. 13}$$

The vapour mass concentration is similar to equations 5 and 6, and is presented in Equation 14.

$$C_v = c_v \overline{m_w} \quad \text{Eq. 14}$$

2.2 Vapour transport equations

The diffusion and convection equation used to describe vapour transport is presented in Equation 15. This is built into the Convection and diffusion application mode in the Chemical Engineering Module. The vapour transport is active inside and outside the porous media using two physics sets. They are linked through their boundary conditions.

$$\frac{\partial c_v}{\partial t} + \nabla \left(D_{v,eff} \nabla c_v \right) = \frac{\dot{m}}{\overline{m_w}} - \nabla \left(c_v u_{g,lin} \right) \quad \text{Eq. 15}$$

This equation requires further expressions to be entered manually as scalar expressions in Comsol. This section presents the terms not previously discussed.

The effective diffusion coefficient is written in Equation 16 according the Bruggeman correction.

$$D_{v,eff} = D_{V,air}\left(\varepsilon S_g\right)^{1.5} \quad \text{Eq. 16}$$

The diffusion coefficient of vapour in air is an empirical relationship. Equation 17 was fitted to the empirical curve.

$$D_{V,air} = -2.775\times10^{-6} + \left(4.479\times10^{-8}\right)T + \left(1.656\times10^{-10}\right)T^2 \quad \text{Eq. 17}$$

The gas linear velocity expression is presented in Equation 18.

$$u_{w,lin} = -\frac{1}{\varepsilon S_g}\frac{\kappa_g}{\eta_g}\nabla P = u\frac{1}{\varepsilon S_g} \quad \text{Eq. 18}$$

2.3 Water transport equations

The diffusion and convection equation used to describe water transport within the porous media is presented in Equation 16. This is built into the Convection and diffusion application mode in the Chemical Engineering Module.

$$\frac{\partial c_v}{\partial t} + \nabla\left(D_{v,eff}\nabla c_v\right) = \frac{\dot{m}}{m_w} - \nabla\left(c_v u_{g,lin}\right) \quad \text{Eq. 19}$$

The capillary diffusion for the water is dependant on the type of food and is therefore not presented in this paper.

The equation for water linear velocity is presented in Equation 20.

$$u_{w,lin} = -\frac{1}{\varepsilon S_w}\frac{\kappa_w}{\eta_w}\nabla P \quad \text{Eq. 20}$$

Permeability is approached in the same manor as for air, the expressions are shown in Equations 21, 22, and 23. S_{ir} = 0.09 in this anlaysis.

$$\kappa_w = \kappa_{wi}\kappa_{wr} \quad \text{Eq. 21}$$

$$\kappa_{wr} = \left(\frac{S_w - S_{ir}}{1 - S_{ir}}\right)^3 \text{ when } S_w > S_{ir} \quad \text{Eq. 22}$$

$$\kappa_{wr} = 0 \text{ when } S_w < S_{ir} \quad \text{Eq. 23}$$

2.4 Oil transport equations

The diffusion and convection equation used to describe oil transport within the porous media is presented in Equation 24. This is built into the Convection and diffusion application mode in the Chemical Engineering Module.

$$\frac{\partial c_o}{\partial t} + \nabla\left(D_{co}\nabla c_o\right) = -\frac{\dot{m}}{m_o} - \nabla\left(c_o u_{o,lin}\right) \quad \text{Eq. 24}$$

Similar to water, the oil capillary diffusion is also is dependant on the type of food and is therefore not presented in this paper.

Evaporation is assumed to be zero. Therefore, there is no source term, and the content of oil within the food remains constant throughout the RF drying process.

The equation for oil linear velocity is presented in Equation 25.

$$u_{o,lin} = -\frac{1}{\varepsilon S_o}\frac{\kappa_o}{\eta_o}\nabla P \quad \text{Eq. 25}$$

Permeability is approached in the same manor as for air, the expressions are presented in Equations 26, 27, and 28. S_{ir} = 0.09 in this anlaysis.

$$\kappa_o = \kappa_{oi}\kappa_{or} \quad \text{Eq. 26}$$

$$\kappa_{or} = \left(\frac{S_o - S_{ir}}{1 - S_{ir}}\right)^3 \text{ when } S_o > S_{ir} \quad \text{Eq. 27}$$

$$\kappa_{or} = 0 \text{ when } S_o < S_{ir} \quad \text{Eq. 28}$$

2.5 Heat transfer equations

The equation used to describe heat transfer is presented in Equation 29. This is built into the Convection and conduction application mode in the Heat Transfer Module.

$$\rho_{eff}C_{p\,eff}\frac{\partial T}{\partial t} = \nabla\left(k_{eff}\nabla T\right) + q - \rho_{eff}C_{p\,eff}u\nabla T \quad \text{Eq. 29}$$

The remaining equations in this section were entered in Comsol as "scalar expressions".

The heat source is provided via RF resistive heating, which is read in from the RF solve. The latent heat loss is subtracted from the RF heating to obtain the total heat input. This expression is presented in Equation 30

$$q = q_{RF} - \lambda_{evap}\dot{m} \qquad \text{Eq. 30}$$

The effective density of the food is calculated using Equation 31

$$\rho_{eff} = (1-\varepsilon)\rho_s + \varepsilon S_g \rho_g + \varepsilon S_w \rho_w + \varepsilon S_o \rho_o$$

Eq. 31

Similarly, the effective heat capacity and thermal conductivity is calculated in Equations 32 and 33 respectively.

$$C_{peff} = (1-\varepsilon)C_{ps} + \varepsilon S_g C_{pg} + \varepsilon S_w C_{pw} + \varepsilon S_o C_{po}$$

Eq. 32

$$k_{eff} = (1-\varepsilon)k_s + \varepsilon S_g k_g + \varepsilon S_w k_w + \varepsilon S_o k_o$$

Eq. 33

2.6 RF equations

The equation used to describe RF is presented in Equation 34. This is built into the In-Plane TE Waves application mode in the Electromagnetic Waves Module.

$$\nabla \times \left(\mu_r^{-1}\nabla \times E\right) = Ek_0^2\left(\frac{\varepsilon_r - j\sigma}{\omega\varepsilon_o}\right)$$

Eq. 34

The loss in the food was calculated using Lichtneckers formula presented in Eq. 35.

$$\varepsilon_c = \varepsilon_s^{(1-\varepsilon)}\varepsilon_o^{\varepsilon S_o}\varepsilon_w^{\varepsilon S_w}\varepsilon_g^{\varepsilon(1-S_o-S_w)} \qquad \text{Eq. 35}$$

Therefore the correct resistive heating is dependant on the individual concentrations of the food constituents.

3. Comsol boundary conditions

There are a number of sophisticated boundary conditions in this model that are worth discussion.

An inlet velocity boundary condition is used for the Navier-Stokes porous media wall. The Darcy wall velocities are used for the vector velocities input in the Navier Stokes boundary conditions. The porous media subdomain is not active in the Navier Stokes physics.

The Darcy Law physics uses Navier Stokes pressure as the boundary condition for the porous media wall. The free flow air domain is not active in the Darcy Law physics.

The vapour convection and diffusion is active in both the porous media domain, and the free flow domain. The porous media reads Darcy's Law velocity vectors in the porous subdomain, and Navier Stokes velocity vectors in the free flow subdomain. The vapour is allowed to escape from the free flow subdomain using a "Convective flux" boundary condition at the airflow outlet.

The water and oil are not allowed to escape from the porous media. Hence, the water volume can only change through evaporation. The oil volume cannot change as no evaporation physics is included for oil.

The heat transfer physics uses similar boundary settings as the vapour convection and diffusion. The heat transfer physics reads Darcy's Law velocity vectors in the porous subdomain, and Navier Stokes velocity vectors in the free flow subdomain.

4. Results for 2D multiphysics model

In this model the RF causes heating, this in turn drives evaporation, which leads to the dehydration of the food. The concentration levels of the water and oil are fed back into the RF analysis via Lichtneckers formula. The purpose of this 2D model was to act as a quick turnaround test bed for sanity checking and for testing future idealisations. Hence the porous media area has a reasonable thickness. The 2D model was run for 500 seconds of transience.

4.1 Electromagnetic Waves results

The geometry used in this analysis was set up for test purposes, and the frequency is 40GHz to avoid cutoff. However, the final 3D moving mesh model will operate at a far lower frequency (between 10MHz and 40MHz).

Similarly, the match is not very important as this model is only used to test the physics. The power input is 200W, however, the energy absorbed by the food at time =0 is only 0.06W. A SPICE circuit will be used on the final 3D model to obtain a well matched RF system.

The electric field at times 0, 250, and 500 seconds is presented in Figure 1, Figure 2, and Figure 3 respectively. The RF field in the multimode cavity changes considerably with time. This is due to evaporation of water. As the food looses moisture, the dielectric constant of the material reduces according to Lichtneckers formula (Equation 35). Therefore, as the moisture reduces, the dielectric constant reduces, and less energy is absorbed by the food. This effect can consequently be used to prevent burning in the RF industrial dryer.

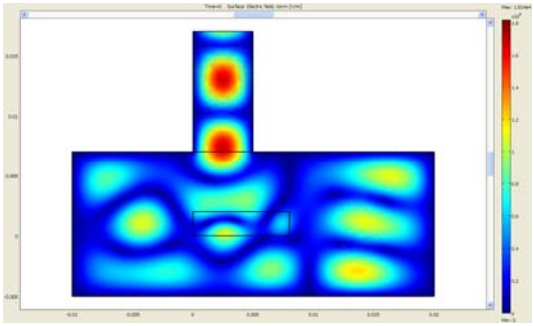

Figure 1 Electric Field at time = 0s

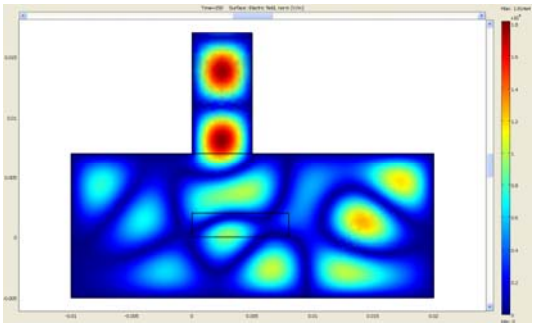

Figure 2 Electric Field at time = 250s

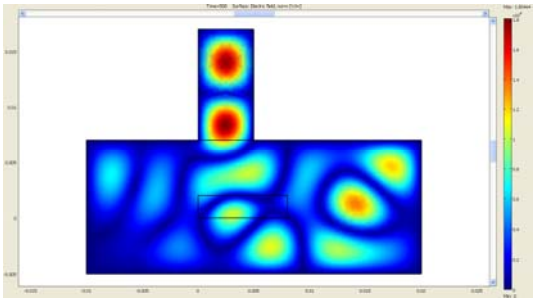

Figure 3 Electric Field at time = 500

The resistive heating at times 0 and 500 seconds is presented in Figure 4 and Figure 5 respectively. The maximum resistive heating reduces from 2.2e7Wm^{-3} down to 1.2e7Wm^{-3} due to the loss in dielectric constant (water removal).

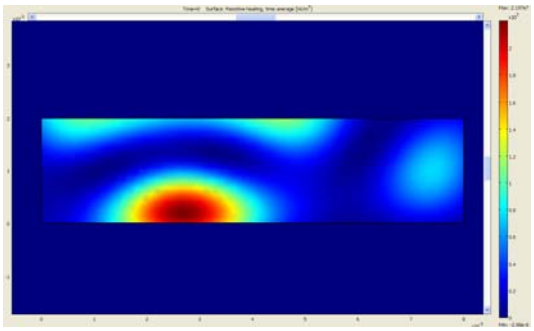

Figure 4 Resistive heating at time = 0

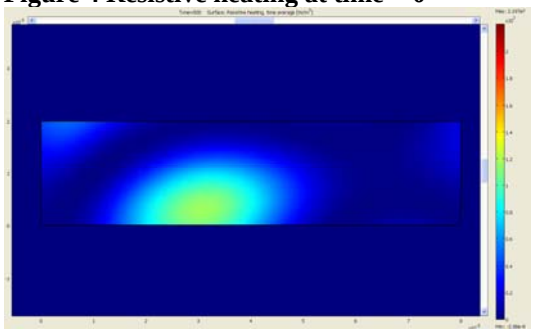

Figure 5 Resistive heating at time = 500

The S11 parameter dB is presented in Figure 6. The S11 parameter gets smaller as the water evaporates from the food. It is interesting that it starts to increase slightly near the end. At this stage, the high electric field in the food domain moves vertically in the y axis, and encounters higher concentrations of water, which causes a change in the RF match.

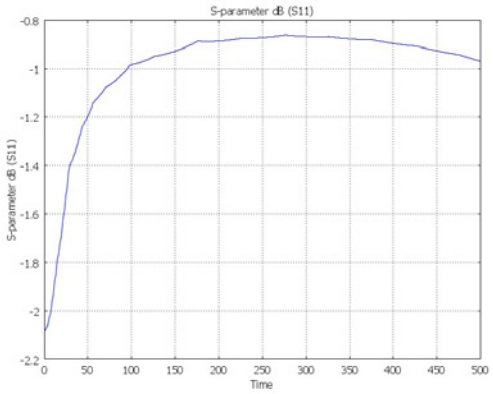

Figure 6 S11 parameter db varying with time

4.2 Navier Stokes and Darcy flow results

The flow inlet is on the left hand side of the free airflow domain, and the outlet is on the right hand side. The fluid flow has an inlet velocity of $3ms^{-1}$. The Navier Stokes and Dacry's Law velocities are presented in Figure 7.

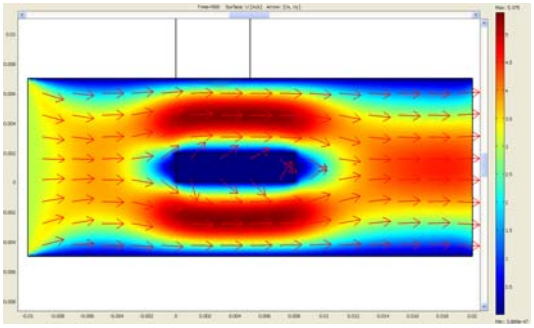

Figure 7 Velocity at time = 500

4.3 Thermodynamic results

Air enters the system from the left hand side of the domain at 60°C. The initial conditions at time = 0 are 60°C with a uniform distribution. Temperature plots at 29 and 500 seconds are presented in Figure 8 and Figure 9 respectively.

The peak temperature occurs at the end of the analysis (500 seconds) near the centre of the porous media. However, the peak temperature near the porous media wall occurs within the first thirty seconds. For example, Figure 10 shows how temperature varies with time at the top right hand corner of the porous media. The peak in temperature at this corner occurs at 29 seconds. This roughly coincides with a peak in vapour production due to high levels of resistive heating.

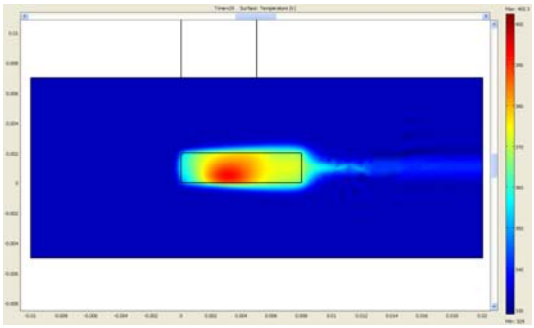

Figure 8 Temperature at time = 29

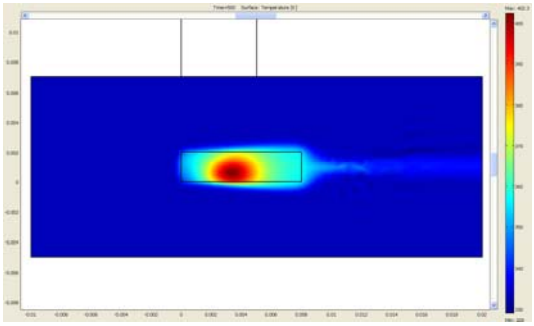

Figure 9 Temperature at time = 500

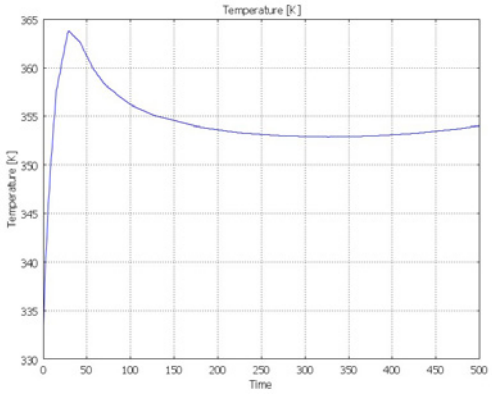

Figure 10 Temperature varying with time

4.4 Vapour results

Vapour production peaks at 29 seconds. After 29 seconds, the loss in water content reduces the dielectric properties of the food, and hence the power input falls sharply. Vapour production at 29 and 200 seconds are presented in Figure 8 and Figure 9 respectively.

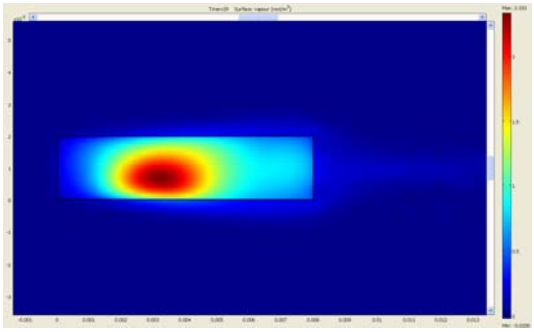

Figure 11 Vapour production at time = 29

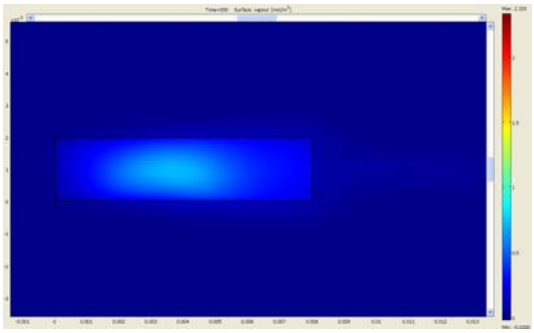

Figure 12 Vapour production at time = 200

Vapour concentration at the top right hand corner of the porous media is presented in Figure 13. It becomes relatively steady state after 200 seconds as the rates of diffusion, evaporation, and heat input stabilise.

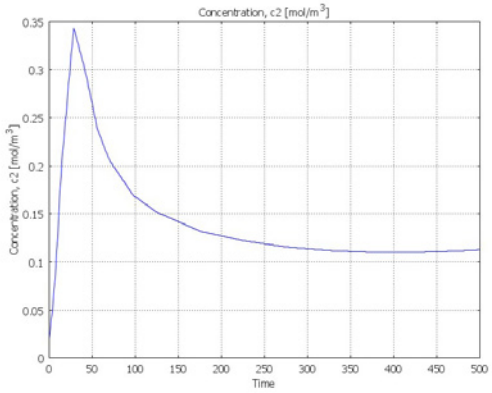

Figure 13 Vapour concentration varying with time

4.5 Oil saturation results

The oil distribution is initially set at 0.2 saturation. This distribution remains constant throughout the 500 seconds of transience. This is predominantly due to the high viscosity of oil and the relatively low pressures experienced.

4.6 Water saturation results

Water Saturation is the most important parameter in this analysis, as the objective is to dehydrate the food, and pump water away from areas of RF heating.

The initial water content was set at 0.2 to ensure darcy's Law takes effect (see equation 23 for cut off). The water saturation at 29, 250, and 500 seconds are presented in Figure 14, Figure 15, Figure 16.

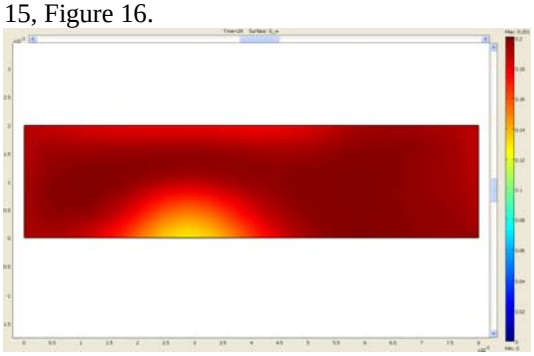

Figure 14 Water saturation at time = 29

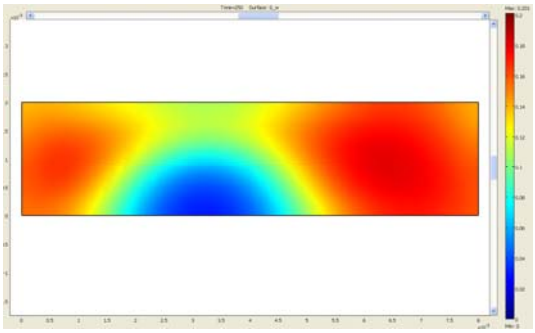

Figure 15 Water saturation at time = 250

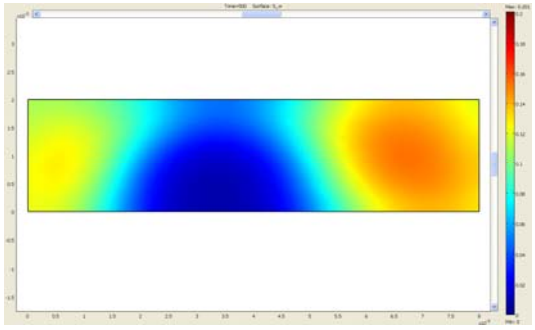

Figure 16 Water saturation at time = 500

The maximum and minimum saturation levels within the porous media are presented in Figure 17. The water saturation in the area of high electric field quite quickly tends towards zero. The maximum saturation line reacts slowly as the water lies outside the area of high electric field, and is dependant on diffusion and Darcy's Law. The real system will have a more even field between electrodes, and the foodstuff will travel through the electric field on a conveyer belt. Therefore, the final system should be effective at evenly dehydrating the food. This analysis demonstrates the fact that diffusion and Darcy's law is relatively slow, and internal heating is required for effective dehydration.

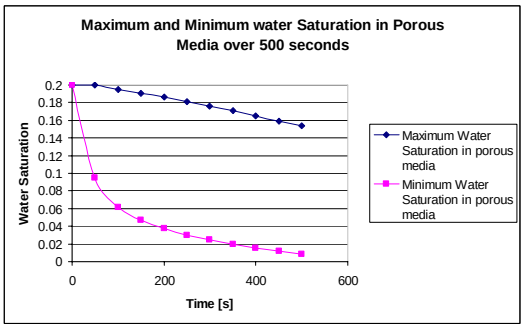

Figure 17 Maximum and minimum water saturation varying with time

4.7 Gas saturation results

Gas saturation levels mirror the water saturation levels as the oil saturation and solid food content remains constant. The gas distribution after 500 seconds is presented in Figure 18.

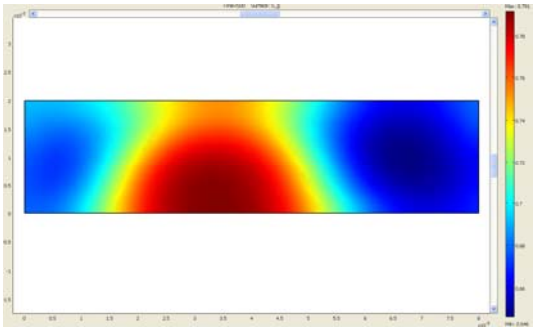

Figure 18 Gas saturation at time = 500

5. Conclusion

Comsol multiphysics can be used to successfully predict water dehydration of porous media foodstuff during RF heating. The RF system reacts to the loss of water through Lichtneckers RF mixture rules. Hence localised heat input will decrease sharply as water content decreases.

This 2D analysis has been used to lay down the architecture of a fully coupled multiphysics model required to describe the industrial RF drying process. It has been used as a test bed to carry out sensitivity studies of material property variance, and idealisation studies.

6. Future work

The critical parameters for the RF industrial dryer can be specified using a large maco/micro environment Comsol Multiphyiscs model. This model can be optimised to ensure dehydration takes place without any burning. Arcing can also be assessed using the final system level model.

Three dimensional models have been consequently built using the same approach discussed in this paper. However, the number of degrees of freedom are enormous due to the number of different physics solving simultaneously. Transient segregated solve techniques must be used in conjunction with appropriate idealisations to model the full industrial process.

8. References

1. Peter Yakubenko, Modelling of drying with Comsol Multiphysics Stage 1. Flow and moisture transport (2008)
2. A. K Datta, Porous media approaches to studying simultaneous heat and mass transfer in food processes II: Property data and representative results, Journal of food engineering 80, pages 96 – 110, (2007)
3. Arun S. Mujumdar, Handbook of Industrial Drying (1995)

9. Acknowledgements

Peter Yakubenko of Comsol worked on this model on a consultancy basis.

10. Nomenclature

Symbol	Parameter	Units
a_w	Water activity	dimensionless
C_o	Oil mass concentration (per unit volume of entire medium)	kgm^{-3}
c_o	Oil concentration	$mol.m^{-3}$
$C_{p\,eff}$	Effective heat capacity of mixture	$Jm^{-3}K^{-1}$
$C_{p\,o}$	Heat capacity of oil	$Jkg^{-1}K^{-1}$
$C_{p\,s}$	Heat capacity of solid food	$Jkg^{-1}K^{-1}$
$C_{p\,w}$	Heat capacity of water	$Jkg^{-1}K^{-1}$
C_v	Vapour mass concentration (per unit volume of entire medium)	kgm^{-3}
c_v	Vapour concentration	$mol.m^{-3}$
C_w	Water mass concentration (per unit volume of entire medium)	kgm^{-3}
c_w	Water concentration	$mol.m^{-3}$
D_{co}	Capillary diffusivity of water	m^2s^{-1}
$D_{v,\,air}$	Diffusion coefficient of vapour in air	m^2s^{-1}
$D_{v,\,eff}$	Effective diffusion coefficient [m^2s^{-1}]	m^2s^{-1}
E	Electric Field	Vm^{-1}
K	Non-equilibrium evaporation constant	dimensionless
k_{eff}	Effective thermal conductivity	$Wm^{-1}K^{-1}$
k_g	Thermal conductivity of gas	$Wm^{-1}K^{-1}$
k_o	Thermal conductivity of oil	$Wm^{-1}K^{-1}$
k_s	Thermal conductivity of solid porous material	$Wm^{-1}K^{-1}$
k_w	Thermal conductivity of water	$Wm^{-1}K^{-1}$
$\dot{m}$	Evaporation	$kg.m^{-3}s^{-1}$
$\overline{m_o}$	Oil molecular weight	$kg.mol^{-1}$
$\overline{m_w}$	Water molecular weight	$kg.mol^{-1}$
P	Pressure	Pa
P_v	Vapour partial pressure	Pa
$P_{v,eq}$	Vapour Equilibrium pressure	Pa
$P_{v,\,sat}$	Vapour saturated partial pressure	Pa
q	Heat source	Wm^{-3}
q_{RF}	RF resistive heating	Wm^{-3}
R	Universal Gas constant	$Jkg^{-1}K^{-1}$
S_g	Gas saturation	dimensionless
S_{ir}	Intrinsic residual saturation	dimensionless
S_o	Oil saturation	dimensionless
S_w	Water saturation	dimensionless
T	Temperature	K
t	Time	s
u	Darcy's velocity	ms^{-1}
$u_{g,lin}$	Gas Linear velocity	ms^{-1}
$u_{o,lin}$	Oil Linear velocity	ms^{-1}
$u_{w,lin}$	Water Linear velocity	ms^{-1}
X_m	Moisture content on dry basis	dimensionless
ε	Porosity	dimensionless
ε_g	Relative Permittivity of gas	dimensionless

ε_o	Relative Permittivity of oil	dimensionless
ε_s	Relative Permittivity of solid food	dimensionless
ε_r	Relative Permittivity of bulk material	dimensionless
ε_w	Relative Permittivity of water	dimensionless
κ_g	Permeability of air in foodstuff	m^2
κ_{gi}	Intrinsic permeability of air	m^2
κ_{gr}	Relative permeability of air	m^2
κ_o	Permeability of oil	m^2
κ_{oi}	Intrinsic permeability of oil	m^2
κ_{or}	Relative permeability of oil	m^2
κ_w	Permeability of water	m^2
κ_{wi}	Intrinsic permeability of water	m^2
κ_{wr}	Relative permeability of water	m^2
λ_{evap}	Latent heat of evaporation of water	$J.kg^{-1}$
η_g	Dynamic viscosity of air	Pa.s
ρ_{eff}	Effective density of mixture	kgm^{-3}
ρ_g	Density of air	kgm^{-3}
ρ_o	Oil density	kgm^{-3}
ρ_s	Density of solid	kgm^{-3}
ρ_w	Water density	kgm^{-3}
σ	Electrical conductivity	Sm^{-1}
μ_r	Relative permeability	dimensionless